

Shapes of the ^{16}N and ^{15}C beta spectra and extraction of matrix elements for $^{15}\text{C}(\beta^-)^{15}\text{N}(\text{g.s.})$

E. K. Warburton, D. E. Alburger, and D. J. Millener
Brookhaven National Laboratory, Upton, New York 11973
(Received 25 January 1984)

The ^{16}N and ^{15}C spectra measured by Alburger, Gallmann, and Wilkinson were reanalyzed to obtain more accurate branching ratios as well as a shape factor for the first-forbidden, nonunique $^{15}\text{C}(\frac{1}{2}^+) \rightarrow ^{15}\text{N}(\frac{1}{2}^-)$ decay. ^{16}N β^- branches were derived to the levels at 0 and 6.13 MeV of 27.9(5)% and 66.3(6)%, respectively; ^{15}C β^- branches were found to ^{15}N levels at 0 and 5.30 MeV of 36.8(8)% and 63.2(8)%, respectively. The ^{15}C shape factor was found to deviate significantly from the allowed shape. Analysis of the shape factor results in the determination of the rank zero component of the transition and determination of the two independent matrix elements which contribute to the rank one component. The possible role of muon capture in determining the rank zero matrix elements is considered. Comparisons, for both the $^{15}\text{C}(\frac{1}{2}^+) \rightarrow ^{15}\text{N}(\frac{1}{2}^-)$ and $^{16}\text{N}(0^-) \rightarrow ^{16}\text{O}(0^+)$ transitions, are made to shell-model calculations with particular emphasis on the sensitivity of the nuclear matrix elements to the choice of the single particle wave function. It is found that rank zero rates calculated with Woods-Saxon wave functions are much smaller than those calculated with harmonic oscillator wave functions. Possible meson-exchange contributions to the rank zero rates are discussed in light of this finding.

I. INTRODUCTION

The $\frac{1}{2}^+$ ground state of ^{15}C decays by β^- emission to ^{15}N with a half-life of 2.449(5) s.^{1,2} The branches to the $\frac{1}{2}^-$ ground state and $\frac{1}{2}^+$ 5299-keV level were determined 25 years ago as 32(2)% and 68(2)%, respectively.¹ Branches to four other excited states were determined by γ -ray spectroscopy and their total is less than 0.1%.²

The relative intensities of the branches to the ground state and 5299-keV level were obtained from a ^{15}C beta-ray spectrum taken with an iron-free intermediate-image magnetic-lens spectrometer. In 1958, when the data were taken at Brookhaven National Laboratory (BNL), there was no computer available for analysis. The spectrum was unfolded into components using a graphical Kurie-plot analysis which also was used to look for deviations from an allowed shape for the two non-negligible components. It was found that the spectra for the β branches to both the $\frac{1}{2}^-$ ground state and $\frac{1}{2}^+$ 5299-keV level had Kurie plots indistinguishable to the eye from allowed shapes. This was felt to be very surprising at the time since the $\frac{1}{2}^+ \rightarrow \frac{1}{2}^-$ β^- decay is nonunique first forbidden and thus would *a priori* be expected to have a nonallowed shape.

The β^- decay of the 2^- ^{16}N ground state to ^{16}O was measured¹ at the same time and using the same apparatus and methods as for ^{15}C . It was found that the branch to the 0^+ ^{16}O ground state had a beta spectrum with a shape in excellent agreement with that expected for this unique first-forbidden decay. This gave considerable added confidence to the ^{15}C results.

Although partially explained by shell-model calculations of Towner and Hardy,³ the reason for the allowed (or nearly allowed) shape for the $^{15}\text{C} \frac{1}{2}^+ \rightarrow \frac{1}{2}^-$ β^- spectrum has remained as somewhat of a puzzle. Interest in

such $J \rightarrow J$ first-forbidden decays was recently revived by Kubodera, Delorme, and Rho.⁴ These authors predicted a large enhancement of the relativistic rank zero matrix element of γ_5 by one-pion exchange. This prediction is based on chiral symmetry and soft-pion theorems and thus its verification would be a rather important check on present models of nucleons and mesons in nuclei. In shell-model calculations,⁵ to investigate this prediction it was found that the rank zero contribution to the total decay rate dominates the rank one and rank two contributions for all the known $J \rightarrow J$ first-forbidden β^- decays in light ($A < 37$) nuclei. This dominance is considerable without the meson exchange contribution (MEC) to the timelike component of the axial current (γ_5) and, furthermore, is enhanced by the expected⁴ MEC of 40–50% in amplitude. Since the rank zero contribution alone deviates negligibly from the allowed shape, one might expect nearly allowed shapes for all $J \rightarrow J$ first-forbidden decays in light nuclei. However, closer examination indicates that this is not necessarily the case. Although the integrated rank one contribution to the decay rate is predicted to be relatively very small, there is a strong cancellation between terms with different energy dependences. The result is a predicted shape factor deviating considerably from allowed.

The strong interest in the MEC to the matrix element of γ_5 led us to reconsider the case of ^{15}C . If the deviation of the shape from the allowed prediction could be extracted accurately enough then the individual rank one matrix elements could be determined as well as the total rank zero contribution to the total decay rate. This would then give a valuable check on the shell-model calculations of the rank one matrix elements as well as a further experimental value for a rank zero decay rate for comparison to calculations with and without MEC. Accordingly, least

squares fits to the 1958 ^{15}C and ^{16}N beta spectrum were undertaken to obtain a more quantitative appraisal of the deviation of the ^{15}C spectrum from the allowed shape. The original measurements and the corrections to them were adequately described in Ref. 1 to which the interested reader is directed for details.

II. ANALYSIS

We will use the following conventions and notation: $\hbar = m_e = c = 1$, W_0 is the electron end point energy, W is the energy of the electron, p is the electron momentum, q is the neutrino momentum, $p = (W^2 - 1)^{1/2}$, $q = W_0 - W$, $F(Z, W)$ is the ratio of the electron density at the nucleus to the density at infinity, and $C(W)$ is the shape factor.

The functional form for the beta spectrum due to a single branch is⁶

$$N(W) = C(W)F(Z, W)pq^2W. \quad (1)$$

The shape factor for an allowed transition is a constant, $C(W) = k$, and for a first-forbidden transition is, to a very good approximation,⁶

$$C(W) = k(1 + aW + b/W + cW^2). \quad (2)$$

If more than one branch is present, then the total spectrum is given by

$$N(W) = \sum_i N_i(W). \quad (3)$$

The partial decay rate for a given branch is proportional to the Fermi function

$$f = \int_1^{W_0} N(W) dW, \quad (4)$$

so that evaluation of f can be done in terms of the integrals

$$I_n = \int_1^{W_0} F(Z, W)pq^2W^{n+1}dW, \quad (5)$$

where, from Eq. (2), $n = 0, 1, -1$, and 2.

The data analysis consisted of a least-squares fit of Eqs. (1)–(3) to the ^{16}N and ^{15}C data. Various portions of the spectra were included in the fit depending on the parameters being determined.

A. $^{16}\text{N}(\beta^-)^{16}\text{O}$

Let us first consider ^{16}N . For a unique first-forbidden transition, the shape factor is given by

$$\frac{1}{12}z^2(p^2 + \lambda_2q^2), \quad (6)$$

where, for the present cases, λ_2 deviates negligibly from unity and z is the rank two nuclear matrix element. Thus, from Eq. (6) we find (omitting the factor $\frac{1}{12}z^2$);

$$k = W_0^2 - 1, \quad ka = -2W_0, \quad kb = 0, \quad kc = 2 \quad (\text{for the } ^{16}\text{N } 2^- \rightarrow 0^+ \text{ decay}). \quad (7)$$

The ^{16}N beta spectrum is shown in Fig. 1. The first fit was made to the portion of the spectrum at higher β^- energies than the end point for any excited state (> 4.5 MeV). The unknowns were k , a , and c . The resulting values for a and c , $-8.99(64) \times 10^{-2}$, and

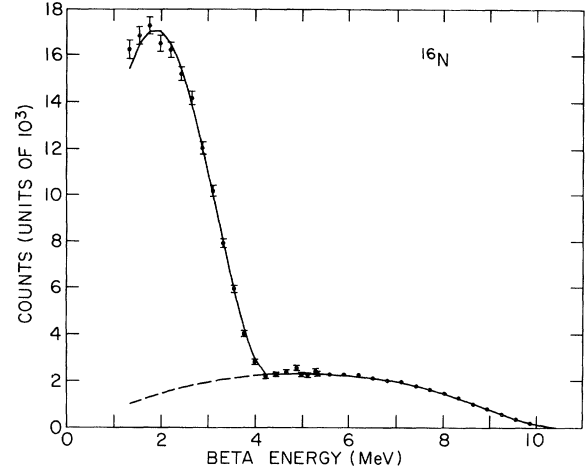


FIG. 1. Beta-ray spectrum for $^{16}\text{N}(\beta^-)^{16}\text{O}$. The data are from Ref. 1. The least squares fit assumed four branches to ^{16}O levels at 0, 6.13, 7.12, and 8.87 MeV and the intensities of the branches to these levels were varied. For the fit shown the uncertainties assigned to the data were adjusted so that the normalized χ^2 was unity. The shape factor for the g.s. branch was fixed at the unique value.

$+4.38(16) \times 10^{-3}$, are in excellent agreement with those predicted by Eq. (7), namely, $a = -9.378 \times 10^{-2}$ and $c = +4.384 \times 10^{-3}$. In this fit the energy calibration of the spectrometer described in Ref. 1 was used. That is, with I the magnet current $p = k_p I$ and k_p was originally determined¹ from calibration points at 0.976 and 2.53 MeV. The $^{16}\text{N}(\beta^-)^{16}\text{O}$ Q value is 10418.6(23) keV, while that for $^{15}\text{C}(\beta^-)^{15}\text{N}$ is 9771.7(8) keV.⁷ These are quite similar. Thus a more accurate calibration at high end-point energy, ~ 10 MeV, for use with the ^{15}C spectrum can be obtained from a fit to the ^{16}N spectrum with the shape factor fixed at the unique value and the spectrometer calibration constant as a variable. Such a fit yielded a calibration 0.36% different from the original one. This calibration was used in all subsequent analysis.

There are four ^{16}N β^- branches intense enough to influence the spectrum of Fig. 1. These are to the g.s. and the 6.13-, 7.12-, and 8.87-MeV levels. A fit to the whole spectrum of Fig. 1 with all four branches was made with the g.s. shape factor fixed as unique and the other three fixed as allowed. This fit, made to test the reliability of the lowest energy portion of the spectrum, yielded branches (in %) to the aforementioned levels of 28.1(6), 66.2(9), 4.8(11), and 1.0(5), respectively. These results are in excellent agreement with the published values⁷ of 26(2), 68(2), 4.9(4), and 1.0(2). The intensities of the β^- branches to the 7.12- and 8.87-MeV states relative to the β^- branch to the 6.13-MeV level were previously determined from the relative intensities of the γ -decay of the levels.⁷ These previous values are more accurate than the present ones from the β spectrum and are adopted in the subsequent analysis to obtain the best ratio of the ground-state branch to the main branch to the 6.13-MeV level. That is, this latter ratio was obtained from a fit to the whole spectrum of Fig. 1 with $I(7.12)/I(6.13)$ and $I(8.87)/I(6.13)$ fixed as explained and $I(\text{g.s.})/I(6.13)$

TABLE I. Beta decay of the ground state of ^{16}N .

Final state		Branch ^a (%)	logft ^b
E_x (MeV)	J^π		
0	0^+	27.9(5)	9.069(5) ^c
6.05	0^+	$1.2(4) \times 10^{-2}$	9.96(15) ^c
6.13	3^-	66.3(6)	4.48(4)
7.12	1^-	4.8(4)	5.11(4)
8.87	2^-	1.0(2)	4.38(9)
9.63	1^-	$1.20(5) \times 10^{-3}$	6.12(5)
9.85	2^+	$6.5(20) \times 10^{-7}$	9.07(13) ^c

^aThe branches to the two ^{16}O levels above 8.87 MeV are not discussed in the text and are from Ref. 7.

^b $T_{1/2} = 7.13(2)$ s, $Q(\beta^-) = 10.419(2)$ MeV.

^c $\log f_{1t}$.

varied. As before, the unique shape factor was assumed for the g.s. branch. The final revised results for the branching ratios in ^{16}N decay are given in Table I. In addition, we find $I(6.13)/I(\text{g.s.}) = 2.36(6)$. These results should replace those in Refs. 1 and 2 and in Table 16.21 of Ref. 7 since these previously published results are based on the original graphical analysis of the data of Fig. 1.

In summary, analysis of the ^{16}N beta spectrum yields the following: (1) shape factor constants for the g.s. branch accurate to $\sim 10\%$ and in excellent agreement with theory; (2) relative branches to the three most intensely fed excited states in excellent agreement with previous determinations (from γ intensities); and (3) a reliable calibration of the spectrometer for use in analysis of the ^{15}C spectrum.

B. $^{15}\text{C}(\beta^-)^{15}\text{N}$

The fit to the ^{15}C spectrum of Fig. 2 was made with four or five unknowns, namely, the intensities of the two non-negligible branches, two constants describing the shape factor [Eq. (2)] and, in some cases, the end-point energy. In principle, the term in b/W should also be included as a variable but this term is essentially negligible except at very low β^- energies. Thus, this term was estimated theoretically and fixed. Surprisingly, the parameters a and c were rather well determined by a fit to the whole spectrum. The value of χ^2 (normalized to the degrees of freedom) was 1.76 with a and c varied and 3.30 with $a=c=0$ (i.e., an allowed shape). The values of a and c from the fit are

$$a = -6.48(90) \times 10^{-2}, \quad c = +2.45(37) \times 10^{-3},$$

$$^{15}\text{C}(\frac{1}{2}^+) \rightarrow ^{15}\text{N}(\frac{1}{2}^-) \quad (8)$$

while the branching ratios for the decays to the g.s. and 5299-keV level are 36.8(8)% and 63.2(8)%, respectively. These are considerably different from the values of 32(2)% and 68(2)% which are the original graphically extracted branching ratios. The principle reason for the difference is the assumption of an allowed shape in the original analysis. The quoted χ^2 values correspond to uncertainties assigned to the individual data points as fol-

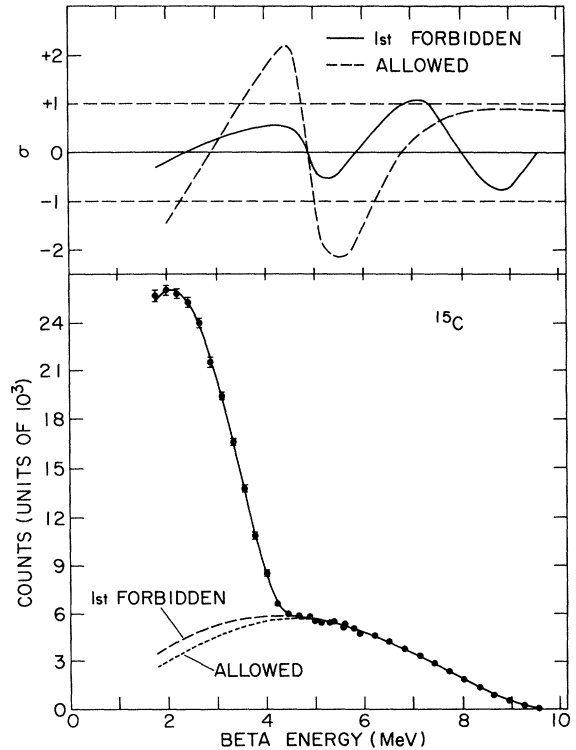


FIG. 2. Beta-ray spectrum for $^{15}\text{C}(\beta^-)^{15}\text{N}$. The data are from Ref. 1. The least squares fit assumed two branches to ^{15}N levels at 0 and 5.30 MeV and the intensities of these branches were varied as was the shape factor for the g.s. branch. The uncertainties assigned to the data were adjusted so that the normalized χ^2 was unity for the forbidden fit.

lows: (1) the counting statistics, (2) the counting statistics in the monitor (relative normalization), and (3) an uncertainty due to possible scattering effects assumed to be $3/E_\beta$ (MeV)%. These uncertainties were added in quadrature. The best values of a and c [Eq. (8)] were obtained with the end-point energy fixed at its known⁷ value of 9771.7(8) keV. However, the uncertainties assigned to a and c (and the branching ratios also) are from a fit with the end-point energy varied as well as a , c , and the relative intensities. This fit gave an end-point energy of 9.763(15) keV in satisfactory agreement with the known value.

The experimental value of f from the definition⁸ $ft = 6170$ s, $t = 2.449(5)$ s,⁷ and the present branching ratio is;

$$f = 928(20) \text{ for } ^{15}\text{C}(\frac{1}{2}^+) \rightarrow ^{15}\text{N}(\frac{1}{2}^-). \quad (9)$$

This completes the information which can be extracted from the data of Fig. 2.

For the scale of Fig. 2, the difference between the allowed and first-forbidden fits is not large enough to be discernible except just above the end point for the branch to the 5299-keV level, i.e., $E_\beta = 4.4-5.0$ MeV. To display the difference and thus the evidence for a non-negligible shape factor, the deviation of the data points (in units of the standard deviation, σ) is displayed for the two fits in

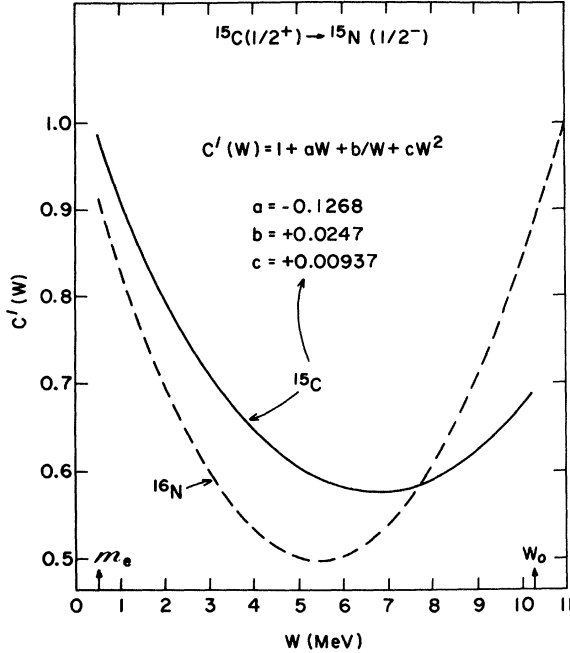


FIG. 3. Shape factor $C'(W) = C(W)/k$ for ^{15}C β decay (solid curve). The constants a and c , in units of MeV^{-1} and MeV^{-2} , respectively, are obtained from a fit to the spectrum, while b is obtained from the matrix elements deduced from the fit together with the theoretical value for w ; see Ref. 8. The shape factor for the unique first-forbidden $^{16}\text{N}(2^-) \rightarrow ^{16}\text{O}(0^+)$ transition is shown for comparison (dashed curve).

the upper part of the figure. The two curves shown here are smoothed representations of the individual points. There is a good deal of scatter about these smoothed curves; however, the correlation of the deviation with energy implied by the curve for the allowed fit is really there. For the forbidden fit, the correlation is weak. Since no energy variation other than that included is expected theoretically, any correlation in the forbidden fit indicates the presence of systematic errors as is also implied by the deviation of χ^2 from unity for the forbidden fit. The error bars in the bottom of Fig. 2 and the values of σ in the upper part correspond to an increase in the calculated uncertainties by $\sqrt{1.76}$, i.e., by χ for the first-forbidden fit. This procedure should cover the indicated systematic (unknown origin) errors. The ^{16}N data ($\chi^2 = 2.5$) were treated similarly.

In summary, the ^{15}C shape factor parameters derived from the 1958 data are found to be significantly different from zero (the shape is not allowed), rather well determined, and roughly half the ^{16}N parameters. The actual shape factors are shown in Fig. 3. We now consider the nuclear structure information extractable from these parameters.

III. EXTRACTION OF MATRIX ELEMENTS

The $^{15}\text{C}(\frac{1}{2}^+) \rightarrow ^{15}\text{N}(\frac{1}{2}^-)$ nonunique first-forbidden transition has contributions from rank zero and rank one matrix elements, i.e., $J_i + J_f < 2$, so rank two cannot parti-

cipate. The f value can be written as

$$f = f^{(0)} + f^{(1)}, \quad (10)$$

where $f^{(R)}$ is the contribution from the R th rank. Given some well-justified approximations, the experimental information available, namely, f , a , and c , is sufficient to determine $f^{(0)}$ and the two independent matrix elements which contribute to $f^{(1)}$. Firstly, we made the $Z\alpha \ll 1$ approximation which gives $\mu_1 = \gamma_1 = \lambda_2 = 1$ in the notation of Schopper.^{6,3,8} This is the approximation used by Warburton, Alburger, and Wilkinson⁹ whose notation we adopt:

$$C(W) = \sum_{M,R} K(MOR)W^M, \quad (11a)$$

$$k = \sum_R K(00R), \quad ka = \sum_R K(10R), \quad kc = \sum_R K(20R). \quad (11b)$$

In Ref. 9, the $K(MOR)$ are given in terms of matrix elements (or combinations of same). As stated previously, the kb/W term in $C(W)$ is practically negligible so that we approximate it by a shell-model derived prediction. The conserved vector current (CVC) is invoked to express the relativistic rank one matrix element $\xi'y$ in terms of the matrix element x (the β -decay analog of the $E1$ operator): $\xi'y = E_\gamma x$ where E_γ is the transition energy for the decay of the ^{15}N $T = \frac{3}{2}$ analog of the ^{15}C g.s. to the ^{15}N g.s. and $E_\gamma = 11.595$ MeV (see the Appendix). Finally, the primed matrix elements x' and u' of Ref. 8 are assumed proportional to the unprimed matrix elements x and u . These primed matrix elements differ from the unprimed ones by an extra factor in the radial integral. Shell-model calculations (Sec. IV) yield $x'/x = 0.73(0.58)$, $u'/u = 0.74(0.62)$ for harmonic oscillator [Woods-Saxon (WS)] single-particle wave functions. The choice made for the constant of proportionality has some effect on the value of x derived from the fit but has little effect on the value of u .

With the above assumptions we have;

$$\begin{aligned} f^{(0)} &= K(000)I_0 + K(-100)I_{-1}, \\ f^{(1)} &= K(001)I_0 + K(101)I_1 + K(201)I_2 \\ &\quad + K(-101)I_{-1}, \\ f &= f^{(0)} + f^{(1)}, \end{aligned} \quad (12)$$

$$k = K(000) + K(001),$$

$$ka = K(101),$$

$$kb = K(-100) + K(-101),$$

$$kc = K(201),$$

and all the $K(MO1)$, which are explicitly defined in Ref. 9, are expressible as quadratics in u and x (the two independent rank one matrix elements). For $^{15}\text{C}(\frac{1}{2}^+) \rightarrow ^{15}\text{N}(\frac{1}{2}^-)$, we have (for WS wave functions);

TABLE II. Results for $^{15}\text{C}(\frac{1}{2}^+) \rightarrow ^{15}\text{N}(\frac{1}{2}^-)$.

Parameter	Present analysis	Shell model ^b		
		$^{14}\text{C}(p, \gamma)^a$	HO	WS
a	$-6.48(90) \times 10^{-2}$		-3.46×10^{-2}	-4.12×10^{-2}
c	$+2.45(37) \times 10^{-3}$		$+1.15 \times 10^{-3}$	$+1.32 \times 10^{-3}$
f	928(20)		993	378
$f^{(0)}$	783(22)		909	272
$f^{(1)}$	145(10)		84	106
x^c	$-0.58(7)$	$\pm 0.58(5)$	-0.58	-0.63
u^c	$-2.68(33)$		-1.80	-1.92

^aSee the Appendix.

^bHarmonic oscillator (HO) and Woods-Saxon (WS) radial wave functions, $1\hbar\omega \rightarrow 0\hbar\omega$ configurational space, and no MEC enhancement. a and c are calculated from the theoretical values for ka and kc and the experimentally derived value for k . See Ref. 8 for details of the calculation.

^cThe relative phase of x and u is determined as even. The overall sign is arbitrary. The matrix elements are in units of fm and are obtained on the assumption that x'/x and u'/u take the calculated WS values. Using HO values yields $x = -0.64$ and $u = -2.67$ with the same errors.

$$\begin{aligned}
 K(001) &= 45.93(u^2 + 5.00ux + 6.41x^2), \\
 K(101) &= -8.74(u^2 + 3.20ux + 1.02x^2) \\
 &= -\frac{4}{3}uY - W_0K(201), \quad (13)
 \end{aligned}$$

$$K(201) = (5u^2 + 4x^2)/9,$$

and

$$\begin{aligned}
 I_0 &= 0.86125, \quad I_1 = 8.6955, \\
 I_{-1} &= 0.10450, \quad I_2 = 100.020, \quad (14)
 \end{aligned}$$

in units of λ_e^{-2} . Using Eqs. (5), (12), (13), and (14), the measured quantities f , a , and c can now be used to solve for $f^{(0)}$, x , and u . Since the $K(M01)$ are quadratics in u and x , there are two solutions; however, one is not physically meaningful ($f^{(0)} < 0$). The results of the physically meaningful solution are summarized in Table II. The calculated WS value $w = -1.76$ can be used to extract $\xi_0 = 30.08$ from $f^{(0)}$ since $K(000) = \xi_0^2 + \frac{1}{9}w^2$, and $K(-100) = -\frac{2}{3}\xi_0 w$. Finally, a breakdown in terms of rank and energy dependence presented in Table III demonstrates the small influence of the kb terms and the strong cancellations occurring in $f^{(1)}$.

IV. THEORY

A. $^{15}\text{C}(\frac{1}{2}^+) \rightarrow ^{15}\text{N}(\frac{1}{2}^-) \beta$ decay

The ^{15}C ground-state wave function is taken from a $1\hbar\omega$ shell-model calculation⁸ and can be written² as

TABLE III. Shape factor and f for $^{15}\text{C} \beta$ decay.

ΔJ	k	ka	kb	kc	
0	905		45.3		
1	790	-110	46.7	4.15	
	kI_0	kaI_1	kbI_{-1}	kcI_2	$f^{(\Delta J)}$
0	779		3.7		783
1	680	-955	4.9	415	145

$^{14}\text{C}(0^+) \times \nu 1s_{1/2}$ with small admixtures of other configurations, the most important of which are $^{14}\text{C}(2^+) \times \nu d_{5/2}$ and $^{14}\text{C}(2^+) \times \nu d_{3/2}$. The ^{15}N ground-state wave function is taken to be simply a $p_{1/2}$ hole configuration.

The rank zero and rank one contributions to the f value are approximately given by

$$f^{(0)} = 0.8613(\xi'v + 8.74w)^2, \quad (15a)$$

$$f^{(1)} = 20.25(10.50x^2 + u^2 - 2.44xu). \quad (15b)$$

From their definitions,⁸ we recall that $\xi'v$, w , x , and u are matrix elements of the operators $i\lambda\vec{\sigma} \cdot \vec{\nabla}/M$, $-i\vec{\lambda} \cdot \vec{\sigma} \cdot \vec{r}$, $-i\vec{r}$, and $-\lambda\vec{r} \times \vec{\sigma}$, respectively, with $\lambda = -c_A/c_V = 1.26$. Of the four nuclear matrix elements, x , u , and the combination $\xi_0 \approx \xi'v + 8.74w$ are determined by fitting the data on $^{15}\text{C} \beta$ decay (Sec. III and Table II).

The one-body density matrix elements (OBDME), in a form appropriate¹⁰ for use with single-particle matrix elements computed with Woods-Saxon wave functions, are given in Table IV. Table IV also gives a breakdown of the contribution to the nuclear matrix elements from each pair of orbits. The calculated values of x and u , slightly larger for the WS case than for the harmonic oscillator (HO) case, are in reasonable agreement with those deduced from the $^{15}\text{C} \beta$ decay data (Table II). However, the deviations from the deduced values are in the opposite direction to our expectations, given that $E1$, $M2$, etc., matrix elements are usually overestimated in calculations restricted to $0\hbar\omega$ and $1\hbar\omega$ spaces.

The most significant difference between the WS and HO matrix elements occurs for $\xi'v$, the matrix element of a derivative operator. Since $\xi'v$ cancels against w in the combination ξ_0 , changes in $\xi'v$ are amplified and the result is a reduction in $f^{(0)}$ by a factor of more than 3 when WS wave functions are used (Table II). To emphasize the point, the behavior of the important $1s_{1/2}-0p_{1/2}$ matrix elements $\xi'v$ and w as a function of binding energy are displayed in Fig. 4 where the strong dependence of $\xi'v$ on the $p_{1/2}$ binding energy is particularly evident. It would require binding energies of ~ 11 and ~ 24 MeV for the $\nu 1s_{1/2}$ and $\pi 0p_{1/2}$ orbits, respectively, to reproduce the

TABLE IV. Matrix elements for $^{15}\text{C}(\frac{1}{2}^+) \rightarrow ^{15}\text{N}(\frac{1}{2}^-)$ β decay.

Quantity	Case	$p_{1/2}1s_{1/2}$	$p_{1/2}d_{3/2}$	$p_{3/2}1s_{1/2}$	$p_{3/2}d_{3/2}$	$p_{3/2}d_{5/2}$	$0s_{1/2}p_{1/2}$	$0s_{1/2}p_{3/2}$	Total
OBDME ^a $\xi'v^a$	$\Delta J=0$	1.0171			-0.0696		-0.0469		
	HO ^b	59.58			-9.12		-3.36		47.10
	WS ^b	45.35			-9.07		-3.47		32.80
8.74 ω	HO	-18.26			2.79		1.03		-14.44
	WS	-19.19			2.80		0.99		-15.39
OBDME x	$\Delta J=1$	1.7617	0.0000	0.0629	0.0555	-0.1929	0.0302	-0.0656	
	HO	-0.957	0.00	0.048	-0.030	0.314	-0.020	0.062	-0.583
	WS	-1.006	0.00	0.049	-0.030	0.316	-0.019	0.060	-0.631
u	HO	-2.413	0.00	-0.061	0.152	0.396	0.051	0.078	-1.797
	WS	-2.536	0.00	-0.062	0.153	0.398	0.049	0.075	-1.923

^aDefined in Ref. 8.

^bHO: $b_0=1.687$ fm, $b_{\text{rel}}=\sqrt{A/A-1}b_0=1.746$ fm; WS: $r_0=r_c=1.40$ fm, $a_0=0.65$ fm, $V_{s_0}=0$. The above parameters reproduce the observed rms charge radius of ^{15}N [2.580(26) fm, Ref. 18] when the procedures of Ref. 10 are followed.

HO matrix elements. However, the actual separation energies¹¹ to the dominant parent, the ^{14}C ground state, are 1.22 and 10.21 MeV. This $p_{1/2}$ binding energy is typical of the values occurring in the evaluation⁵ of $1s_{1/2}$ - $0p_{1/2}$ matrix elements in the mass region $11 \leq A \leq 21$. To reproduce the observed $f^{(0)}$ an enhancement factor to $\xi'v$ of 1.4 is required, in line with expectations^{12,13} for pion exchange-current contributions.

B. $^{16}\text{N}(0^-) \rightarrow ^{16}\text{O}(0^+) \beta$ decay

It is interesting to compare the ^{15}C β decay with the much studied¹² $^{16}\text{N}(0^-) \rightarrow ^{16}\text{O}(0^+)$ transition to which,

from the point of view of nuclear structure, it is very similar. For ^{16}N decay

$$f^{(0)} \approx 1.264(\xi'v + 9.43w)^2. \quad (16)$$

The experimental value¹⁴ is $f = f^{(0)} = (4.02 \pm 0.40) \times 10^3$. Using the $1\hbar\omega$ and $0\hbar\omega$ initial and final $A=16$ wave functions, the HO (WS) values of $\xi'v$, $9.43w$, and $f^{(0)}$ are -70.87 (-57.35), 25.60 , (30.05) , and 2546 (949). Again, the use of single-particle wave functions more realistic than HO wave functions leads to a substantial reduction in $f^{(0)}$; in the WS case, $\xi'v$ needs to be enhanced by a factor of 1.5 to reproduce the experimental value of $f^{(0)}$. A larger enhancement factor is anticipated for an expanded shell-model space since $2\hbar\omega$ admixtures have been shown¹² to reduce $f^{(0)}$; a similar effect is expected for $A=15$.

C. Muon capture on ^{15}N

In muon capture, the equivalents of the β -decay matrix elements $\xi'v$ and w enter with a relative sign that is opposite to that for the β -decay process, a fact which has been exploited in the study¹² of the $^{16}\text{N}(0^-) \rightarrow ^{16}\text{O}(0^+)$ transition. Since it is possible to study experimentally μ capture on ^{15}N leading to the particle stable ground state ($\frac{1}{2}^+$) and first excited state ($\frac{5}{2}^+$) of ^{15}C , it is of interest to calculate the expected capture rates.

We calculate the partial capture rates using the formalism of O'Connell, Donnelly, and Walecka^{15,16} except that we choose $F_A^\beta(0) = F_A^\mu(0) = -1.26$ to be consistent with the value we use for β decay. Other relevant parameters are the neutrino energy, 94.91 and 94.17 MeV for transitions to the $\frac{1}{2}^+$ and $\frac{5}{2}^+$ final states, respectively, and the square of the muon wave function averaged over the nucleus,

$$|\phi_{1s}|_{aV}^2 = 40.36 \text{ MeV}^3. \quad (17)$$

The reduction factor $R=0.825$ used to get $|\phi_{1s}|_{aV}^2$ was obtained by averaging the ^{12}C and ^{16}O values from Table 3 of Ref. 16.

The calculated capture rates are given in Table V for both HO and WS cases and also for WS with a 40% enhancement of the rank zero matrix element of the time-

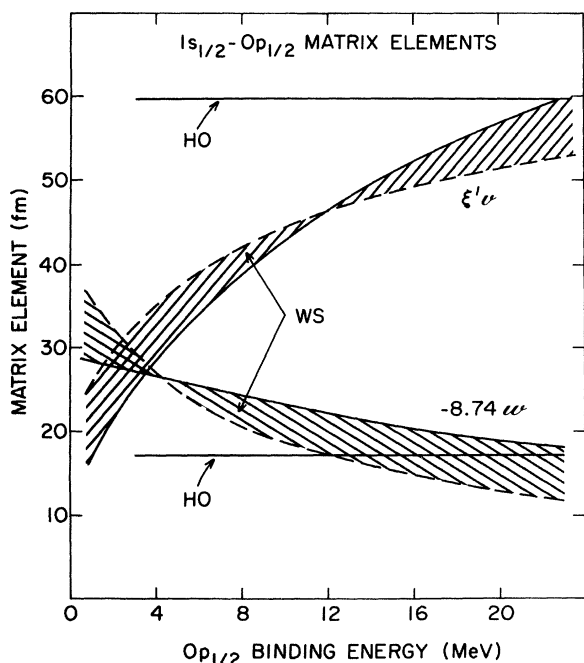


FIG. 4. The nuclear matrix elements $\xi'v$ and $-8.74w$, as a function of single-particle binding energy for the $1s_{1/2}$ and $0p_{1/2}$ orbits. The dashed and solid curves are for $1s_{1/2}$ binding energies of 1 and 13 MeV, respectively. The rank zero contribution to the $\frac{1}{2}^+ \rightarrow \frac{1}{2}^-$ β -decay rate is proportional to the square of the difference between the two matrix elements and varies rapidly as a function of the $0p_{1/2}$ binding energy.

TABLE V. Calculated partial muon capture rates for ^{15}N .

Final state	Case	ω_-^a	ω_+^a	ω^b
$\frac{1}{2}^+$	HO	0.578	0.773	1.350
	WS	0.324	0.561	0.885
	c	0.439	0.561	1.000
$\frac{5}{2}^+$	HO	3.71	0.04	3.75
	WS	3.63	0.08	3.71

^a ω_{\pm} is the contribution to the capture rate from rank $J_f \pm \frac{1}{2}$ matrix elements.

^b $\omega = \omega_+ + \omega_-$ is the partial capture rate in units of 10^3 s^{-1} .

^cWS with the timelike matrix element enhanced by a factor of 1.4.

like current. We note that: (i) in contrast to β decay, the rank one contribution to the $\frac{1}{2}^- \rightarrow \frac{1}{2}^+$ transition is larger than the rank zero contribution; (ii) the rank zero and rank one matrix elements are sensitive to the radial wave functions; (iii) it is possible that the $\frac{1}{2}^- \rightarrow \frac{5}{2}^+$ rate is overestimated since the analogous $0^+ \rightarrow 2^-$ transition rate for μ capture on ^{16}O is overestimated by a factor of 2 when the wave functions are restricted to $0\hbar\omega$ and $1\hbar\omega$; and (iv) it appears unlikely that a conventional μ capture experiment could be used to obtain useful information on the $\frac{1}{2}^- \rightarrow \frac{5}{2}^+$ transition since this rate would presumably be obtained from a difference between the total capture rate to bound states and the capture rate for the stronger $\frac{1}{2}^- \rightarrow \frac{3}{2}^+$ transition.

For $^{16}\text{O} + \mu^- \rightarrow ^{16}\text{N}(0^-)$, we obtain $w = 2.03 \times 10^3 \text{ s}^{-1}$ and $1.41 \times 10^3 \text{ s}^{-1}$ for HO and WS wave functions, respectively; enhancing the time component in the WS case by a factor of 1.5 yields $w = 2.11 \times 10^3 \text{ s}^{-1}$. The experimental value¹⁷ is $w = (1.56 \pm 0.11) \times 10^3 \text{ s}^{-1}$. Although the μ capture rates are sensitive to the choice of radial wave function, the sensitivity is not as strong as for the inverse β decay, where the effects are magnified by the cancellation between the contributions of the timelike and spacelike currents to the matrix element.

V. CONCLUSIONS

The $^{15}\text{C}(\frac{1}{2}^+) \rightarrow ^{15}\text{N}(\frac{1}{2}^-)$ β spectrum has been found to differ significantly from an allowed shape. An analysis of the $^{16}\text{N}(2^-) \rightarrow ^{16}\text{O}(0^+)$ β spectrum, a transition with a similar end point and a known shape factor, gives considerable confidence in the results from the ^{15}C analysis. The ^{15}C analysis yields (i) a ground state branching ratio for the β decay and hence the f value for the ground state transition, (ii) the division of f into $f^{(0)}$ and $f^{(1)}$, and (iii) the two rank one matrix elements which determine $f^{(1)}$ and the shape factor. The value obtained for the $E1$ -type matrix element x is consistent with a value deduced from the analog γ decay in ^{15}N (see Appendix). Our shell-model calculations reproduce the observed value for x but somewhat underestimate the value of u .

The value of $f^{(0)}$ determines a linear combination ξ_0 of the two rank zero matrix elements $\xi'v$ and w , a quantity

of interest since one-pion exchange currents are expected to contribute significantly to $\xi'v$. The important result of the present calculations is that it is very important to calculate the one-body contribution to $\xi'v$, i.e., the matrix element of γ_5 , using realistic single-particle wave functions. The $\xi'v$ matrix elements for ^{15}C , $^{16}\text{N}(0^-)$, and the previously studied⁸ ^{11}Be decay are considerably smaller when calculated with Woods-Saxon wave functions than if harmonic oscillator wave functions are used, leading, in the impulse approximation to very much smaller values for $f^{(0)}$. The same is true for all the nine cases studied in Ref. 5, as might be surmised from Fig. 4 since the $1s_{1/2}-0p_{1/2}$ matrix element dominates in all cases. It is clear that the use of harmonic oscillator wave functions in previous calculations^{12,13} overestimates the rank zero contribution in the impulse approximation and these calculations should be reconsidered.

For ^{15}C and $^{16}\text{N}(0^-)$ β decay, where the nuclear structure is simplest ($1s_{1/2}-0p_{1/2}$ contribution most dominant), meson exchange contributions to $\xi'v$ at a level of 40–50% of the impulse approximation matrix element would give agreement with the measured $f^{(0)}$. However, we have yet to consider $2\hbar\omega$ (and higher) correlations in both the initial and final states. Such correlations are expected to further reduce the calculated value of $f^{(0)}$.

APPENDIX: RADIATIVE WIDTH OF THE $^{15}\text{N} 11.595 \rightarrow 0$ TRANSITION

The β matrix element x can also, in principle, be extracted from the radiative width Γ_{γ_0} for the ground-state decay of the ^{15}N analog of the ^{15}C ground state. In this appendix we consider the extraction of a value of x from $^{14}\text{C}(p, \gamma_0)^{15}\text{N}$ data. There are two problems to be discussed. First, the evaluation of Γ_{γ_0} from the available experimental^{19–22} and theoretical^{23–25} reports is somewhat complicated and has not been done by the compilers.^{7,26}

TABLE VI. $^{14}\text{C}(p, \gamma_0)^{15}\text{N}$ cross section measurements for $E_p = 1.50 \text{ MeV}$.

Cross section ($\mu\text{b}/\text{sr}$)	Accuracy (%)	Reference
7.7	20	19, 24 ^a
17.5	40	20
17.5	16	21, 22 ^b
16.8	25	22
17.3	13	Weighted average of last 3

^aThe cross section can be derived from information contained in Ref. 19 but is not given explicitly. The quoted cross section is taken from Fig. 2 of Ref. 24. The quoted uncertainty is from Ref. 19.

^bThis is not a direct measurement. The yield curves of Refs. 20 and 21 overlap at a $E_p = 2.48\text{-MeV}$ resonance where they agree perfectly. This agreement constitutes an independent calibration of the absolute cross section scale of Ref. 20.

TABLE VII. Resonance energies and radiative widths from Ref. 25. [All energies are in the center-of-mass system. The uncertainties in the last figure (in parentheses) represent the spread in the individual results for the two theories and for average (1) they represent the spread between the R matrix and S matrix averages. Average (2) includes the experimental uncertainties added in quadrature. These are the adopted values.]

Theory	E_p (MeV)		Γ_{γ_0} (eV) ^a	
	$T = \frac{1}{2}$	$T = \frac{3}{2}$	$T = \frac{1}{2}$	$T = \frac{3}{2}$
R matrix	1.236(1)	1.429(8)	7.5(3)	48.4(8)
S matrix	1.238(1)	1.346(3)	4.6(1)	50.7(40)
Average (1)	1.237(1)	1.388(40)	6.1(15)	49.6(12)
Average (2)	1.237(3)	1.388(40)	6.1(17)	49.6(65)

^aThe radiative widths of Ref. 19 have been scaled upwards by 2.1 as discussed in the text.

Second, there is interference between the J^π , $T = \frac{1}{2}^+$, $\frac{3}{2}$ analog at ~ 11.6 MeV and a nearby $\frac{1}{2}^+$, $\frac{1}{2}$ resonance at 11.4 MeV. This interference causes isospin mixing between the two levels which will affect the value of Γ_{γ_0} (and thus x). Thus, we consider an estimation of the “zero-order” value of Γ_{γ_0} , i.e., the value which would have pertained in the absence of the mixing. The radiative width Γ_{γ_0} is evaluated from the $^{14}\text{C}(p,\gamma_0)^{15}\text{N}$ cross section at the peak of the $E_p = 1.50$ -MeV resonance corresponding to the 11.6-MeV level. Four measurements of this cross section are listed in Table VI. The last three are in excellent agreement but differ from the first by an average factor of 2.25. Thus we discard the first and adopt the weighted average of the last three.

The interference between the 11.6-MeV level ($E_p = 1.50$ MeV) and the 11.4-MeV level ($E_p = 1.31$ MeV) has provided a popular experimental test of multilevel compound nucleus theories. Three reports have been published of simultaneous fits to the yield curves for the $^{14}\text{C}(p,\gamma_0)$ and $^{14}\text{C}(p,n)$ reactions. These all used the $^{14}\text{C}(p,\gamma_0)^{15}\text{N}$ data of Bartholomew *et al.*¹⁹ which, as discussed, we conclude has a cross section a factor of 2.25 times too small. However, the analysis can simply be scaled by this factor.²⁷

The three analyses were performed by Ferguson and Gove²³ in 1959, French, Iwao and Vogt²⁴ in 1961, and Tindle and Vogt²⁵ in 1969. The analysis became more so-

phisticated and comprehensive with time and we need only consider the last one. Tindle and Vogt considered three different R -matrix fits and two different S -matrix fits. The results within each theory were very similar and can be averaged. We present a summary of the radiative widths resulting from the two theories in Table VII. We adopt the bottom line [average (2)] for the two levels. Using a (p,γ) Q value of 10.2074 MeV,⁷ the two $\frac{1}{2}^+$ levels are at excitation energies of 11444(3) and 11595(40) keV, respectively. We note that the uncertainties in the theoretical analysis are rather large for the excitation energy of the broad [$\Gamma_{\text{tot}} = 485(10)$ keV (Ref. 25)] $T = \frac{3}{2}$ level and for Γ_{γ_0} in the case of the $T = \frac{1}{2}$ level but small for the energy of the $T = \frac{1}{2}$ level and the radiative width of the $T = \frac{3}{2}$ level.

Assuming isospin conservation, the β matrix element x is related to Γ_{γ_0} for the $T = \frac{3}{2}$ level by⁸

$$|x| = [4\pi B(E1)]^{1/2}; \quad \Gamma_{\gamma_0} = 1.04653 E_\gamma^3 B(E1), \quad (\text{A1})$$

with E_γ in MeV, and Γ_{γ_0} in eV. Before applying Eq. (A1) we estimate the effect of the isospin mixing between the two $\frac{1}{2}^+$ levels. This problem was considered in detail by French *et al.*²⁴ They argued that other levels could be ignored and the isospin impurity in the two levels could be directly related to the ratio of their reduced neutron widths since a $T = \frac{3}{2}$ level cannot neutron decay to a $T = 0$ level (^{14}N g.s.). The calculated admixture is then 5.0% for the R -matrix calculation and 2.8% for the S -matrix calculation. Using the procedure described by French *et al.*, the estimation of the “zero-order” radiative widths is straightforward. The experimental results of Table VII yield zero-order widths of 19 and 41 for the R -matrix calculation and 12 and 48 for the S -matrix calculation. We adopt

$$\begin{aligned} \Gamma_{\gamma_0}(T = \frac{1}{2}) &= 16(4) \text{ eV}, \\ \Gamma_{\gamma_0}(T = \frac{3}{2}) &= 44(7) \text{ eV} \end{aligned} \quad (\text{A2})$$

(adopted “zero-order” values).

From Eq. (A1), the $T = \frac{3}{2}$ radiative width corresponds to $|x| = 0.58(5)$.

This research was supported by the U. S. Department of Energy, Division of Basic Energy Sciences, under Contract No. DE-AC02-76CH00016.

¹D. E. Alburger, A. Gallmann, and D. H. Wilkinson, *Phys. Rev.* **116**, 939 (1959).

²D. E. Alburger and D. J. Millener, *Phys. Rev. C* **20**, 1891 (1979).

³I. S. Towner and J. C. Hardy, *Nucl. Phys.* **179**, 489 (1972).

⁴K. Kubodera, J. Delorme, and M. Rho, *Phys. Rev. Lett.* **40**, 755 (1978).

⁵D. J. Millener and E. K. Warburton (unpublished); E. K. Warburton, *Bull. Am. Phys. Soc.* **28**, 726 (1983).

⁶H. Schopper, *Weak Interactions and Nuclear Beta Decay* (North-Holland, Amsterdam, 1966).

⁷F. Ajzenberg-Selove, *Nucl. Phys.* **A375**, 1 (1982).

⁸D. J. Millener, D. E. Alburger, E. K. Warburton, and D. H.

Wilkinson, *Phys. Rev. C* **26**, 1167 (1982).

⁹E. K. Warburton, D. E. Alburger, and D. H. Wilkinson, *Phys. Rev. C* **26**, 1186 (1982).

¹⁰D. J. Millener, J. W. Olness, E. K. Warburton, and S. S. Hanna, *Phys. Rev. C* **28**, 497 (1983).

¹¹F. Ajzenberg-Selove, *Nucl. Phys.* **A360**, 1 (1981).

¹²I. S. Towner and F. C. Khanna, *Nucl. Phys.* **A372**, 331 (1981), and references contained therein.

¹³E. G. Adelberger, M. M. Hindi, C. D. Hoyle, H. E. Swanson, R. D. Von Lintig, and W. C. Haxton, *Phys. Rev. C* **27**, 2833 (1983).

¹⁴The quoted $f^{(0)}$ [equivalent to $\Lambda_\beta = 0.452(45) \text{ s}^{-1}$] is obtained by averaging the beta decay rate $\Lambda_\beta = 0.45(5)$ of C. A.

- Gagliardi, G. T. Garvey, J. R. Wrobel, and S. J. Freedman, *Phys. Rev. C* **28**, 2423 (1983), with an updated value $\Lambda_\beta=0.46(10)$ of L. Palfy, J. P. Deutsch, L. Grenacs, J. Lehmann, and M. Steels, *Phys. Rev. Lett.* **34**, 212 (1975), quoted by Gagliardi *et al.* A preliminary result $\Lambda_\beta=0.54(8)$ of L. A. Hamel, L. Lessard, J. Chauvin, and H. Jérémie, *Bull. Am. Phys. Soc.* **28**, 40 (1983), is consistent with the above result but a recent result, $\Lambda_\beta=0.60(7)$ of T. Minamisono, K. Takeyama, T. Ishigai, H. Takeshima, Y. Nojiri, and K. Asahi, *Phys. Lett.* **130B**, 1 (1983), disagrees with the earlier measurements.
- ¹⁵J. S. O'Connell, T. W. Donnelly, and J. D. Walecka, *Phys. Rev. C* **6**, 719 (1972).
- ¹⁶J. D. Walecka, in *Muon Physics*, edited by V. W. Hughes and C. S. Wu (Academic, New York, 1975).
- ¹⁷P. Guichon, B. Bihoreau, M. Giffon, A. Goncalves, J. Julien, L. Roussel, and C. Samour, *Phys. Rev. C* **19**, 987 (1979).
- ¹⁸W. Schütz, *Z. Phys. A* **273**, 69 (1975).
- ¹⁹G. A. Bartholomew, F. Brown, H. E. Gove, A. E. Litherland, and E. B. Paul, *Can. J. Phys.* **33**, 441 (1955).
- ²⁰H. M. Kuan, C. J. Umbarger, and D. G. Shirk, *Nucl. Phys.* **A160**, 211 (1971); **A196**, 634 (1972).
- ²¹F. C. Young, A. S. Figuera, and C. E. Steerman, *Nucl. Phys.* **A173**, 239 (1971).
- ²²M. H. Harakeh, P. Paul, H. M. Kuan, and E. K. Warburton, *Phys. Rev. C* **12**, 1410 (1975).
- ²³A. J. Ferguson and H. E. Gove, *Can. J. Phys.* **37**, 660 (1959).
- ²⁴J. B. French, S. Iwao, and E. Vogt, *Phys. Rev.* **122**, 1248 (1961).
- ²⁵C. T. Tindle and E. Vogt, *Can. J. Phys.* **47**, 2763 (1969).
- ²⁶P. M. Endt, *At. Data Nucl. Data Tables* **23**, 3 (1979).
- ²⁷Actually a factor of 2.1 is used due to slight differences in the present treatment of $\sigma(p, \gamma_0)$ here and in Ref. 25.